PFC Control Signal Driven MPPT Technique for Grid-Connected PV Systems

Luigi Costanzo, Guido Rubino, *Member, IEEE*, Luigi Rubino, and Massimo Vitelli

***Abstract*—In this article, a novel MPPT technique is proposed and experimentally tested. It is called "grid-connected photovoltaic (PV) systems maximum power point tracking (MPPT) technique driven by the power factor correction (PFC) controller" (CICERONE). It generates, for both single stage (SS) and double stage (DS) grid-connected PV systems, the bulk voltage reference by exploiting only the internal (not coming from sensors) PFC control signal. CICERONE leads to a piecewise ramp bulk voltage whose slope is updated to maximize the average power injected into the grid. Experimental results show that CICERONE exhibits better performance and robustness than the Perturb and Observe MPPT technique, especially in case of dynamic irradiance conditions. In addition, CICERONE can be applied without modifications to both SS and DS grid-connected PV systems. Hence, differently from a traditional DS system, in a CICERONE based DS system, the dc–dc converter can be operated with a fixed duty-cycle and can work in the highest efficiency conditions. Moreover, CICERONE operates without using external signals coming from sensors and affected by measuring noise (such as PV voltage, PV current, grid current, or their derivatives), but it performs the MPPT using only an internal signal already used for PFC purposes.**

***Index Terms*—Grid-connected systems, maximum power point tracking, photovoltaic.**

I. Introduction

PHOTOVOLTAIC (PV) systems represent one of the most important solutions to face the renewable energy demand of the next years [1], [2], [3]. The connection of PV arrays to the utility grid is implemented by means of grid-connected PV systems (GPVSs). Important features of GPVSs are power factor correction (PFC) and maximum power point tracking (MPPT). In order to carry out such important features, single stage GPVSs (SS-GPVSs) and double stage GPVSs (DS-GPVSs) are usually employed [4], [5], [6], [7], [8], [9].

In both SS-GPVSs and DS-GPVSs a dc–ac converter, used in order to couple the PV array with the grid, is equipped with a wide-bandwidth grid current controller that performs the PFC on the ac side [10], [11]. Moreover, an energy-storage bulk capacitor bank is placed at the dc side of the inverter for ensuring the balance between the PV dc power and the average ac power injected into the grid. To this aim, a low-bandwidth controller is employed for regulating the bulk capacitor voltage and, at the same time, allowing its oscillations at the second harmonic of the grid frequency [12].

As concerns the MPPT feature, as it is shown in Fig. 1(a), in a traditional SS-GPVS the PV array is directly connected to the inverter and, hence, the MPPT control is carried out regulating

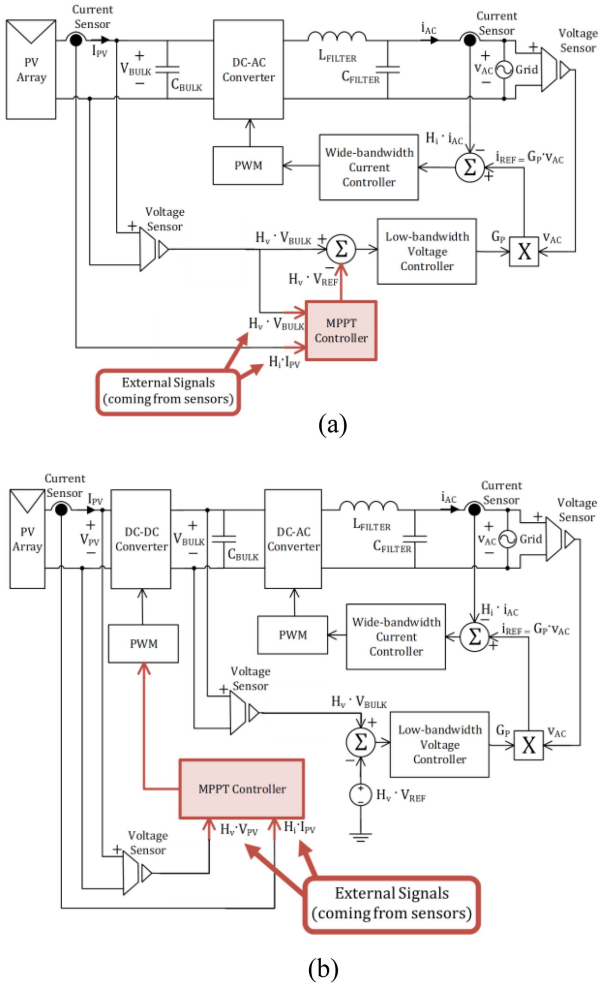

Fig. 1. (a) Traditional SS-GPVS and (b) traditional DS-GPVS. The input signals of the MPPT controllers are external (coming from sensors).

Manuscript received 5 December 2023; revised 19 February 2024; accepted 20 April 2024. Date of publication 24 April 2024; date of current version 20 June 2024. This work was supported by the Università degli Studi della Campania Luigi Vanvitelli in the framework of "Piano Strategico di Ateneo 2021–2023—Azione strategica R1.S2" under Grant SCAVENGE. Recommended for publication by Associate Editor D. M. Xu. *(Corresponding author: Luigi Costanzo.)*

Luigi Costanzo, Luigi Rubino, and Massimo Vitelli are with the Department of Engineering, Università degli Studi della Campania "Luigi Vanvitelli," 81031 Aversa, Italy (e-mail: luigi.costanzo@unicampania.it; luigi.rubino@unicampania.it; massimo.vitelli@unicampania.it).

Guido Rubino is with the Department of Astronautical, Electrical, and Energy Engineering, University of Rome "La Sapienza," 00184 Rome, Italy (e-mail: guido.rubino@uniroma1.it).

Color versions of one or more figures in this article are available at https://doi.org/10.1109/TPEL.2024.3393294.

Digital Object Identifier 10.1109/TPEL.2024.3393294

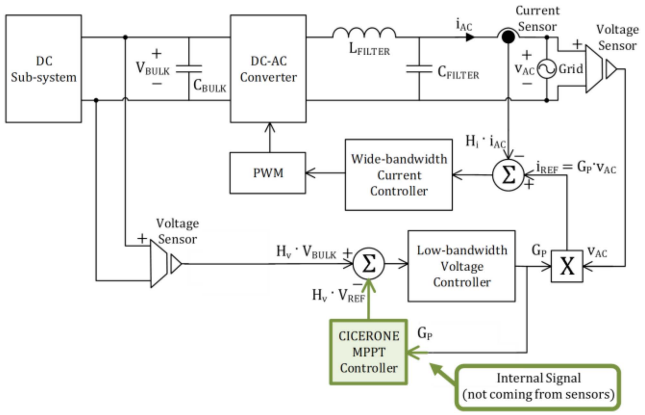

Fig. 2. CICERONE based SS-GPVS or DS-GPVS. The only input of CICERONE MPPT controller is the internal (not coming from sensors) PFC signal G_P.

the bulk voltage that is coincident with the PV array voltage. Instead, in a traditional DS-GPVS, as it is shown in Fig. 1(b), a dc–dc converter is placed between the PV array and the inverter. Therefore, the MPPT control is carried out by regulating the PV voltage that is decoupled from the bulk voltage. Hence, in a traditional SS-GPVS, the reference signal for the bulk voltage, coincident with the PV voltage, is time-varying and is generated by the MPPT controller. In a traditional DS-GPVS, while the reference signal for the PV array voltage is time-varying and is generated by the MPPT controller, the reference signal for the bulk voltage is fixed [12]. Hence, in a traditional DS-GPVS the dc–dc converter duty cycle and the corresponding voltage conversion ratio are time-varying.

A great number of MPPT techniques has been presented and discussed in the literature with the aim of identifying the optimal reference signal for the PV array voltage both in SS-GPVSs and DS-GPVSs. Among them, the Perturb and Observe (P&O) technique has emerged as one of the simplest but nonetheless more efficient MPPT techniques and is widely accepted as a benchmark MPPT technique [12], [13], [14], [15], [16]. In standard SS-GPVSs and DS-GPVSs equipped with P&O MPPT controllers, the reference signal for the PV voltage is identified by using the external (that is coming from sensors) information on the PV current and the PV voltage for tracking the maximum PV extracted power. In [16], a novel MPPT technique with a tracking efficiency comparable to that of the P&O has been proposed and numerically tested. With respect to the P&O, it does not need the detection of the PV current, and it automatically takes into account the dc–ac power stage efficiency profile [17]. However, it has been specifically designed only for SS-GPVSs and, in addition, it requires the computation of the time-derivative of the PV voltage.

In this article, grid-connected photovoltaic (PV) systems maximum power point tracking (MPPT) technique driven by the power factor correction (PFC) controller. It is able to generate, for both SS-GPVSs and DS-GPVSs, the bulk capacitor voltage reference V_{REF} by exploiting only the PFC control signal, which is the internal (not coming from sensors) signal G_P at the output of the "low-bandwidth voltage controller". CICERONE leads to a V_{REF} waveform characterized by a piecewise ramp profile whose slope is updated in order to maximize the average power injected into the grid.

The investigation discussed in this article demonstrates that CICERONE exhibits better performance and robustness, especially in case of dynamic irradiance conditions, with respect to the benchmark P&O technique. In addition, CICERONE is characterized by the following salient specific features, which fully justify its novelty.

1) It can be applied without modifications to both SS-GPVSs and DS-GPVSs.
2) Differently from a traditional DS-GPVS, in a CICERONE based DS-GPVS, the dc–dc converter can be operated at a fixed duty-cycle and, hence, it is allowed to permanently work in its highest efficiency operating conditions, which is at a fixed predetermined voltage conversion ratio coincident with that characterized by the highest power stage efficiency [18].
3) CICERONE automatically involves the maximization of the average power injected into the grid instead that the maximization of the power extracted by the PV array. It is intuitive to understand that MPPT techniques aimed at the maximization of the power extracted by the PV array do not automatically lead to the maximization of the power injected into the grid due to the shape of the profile of the conversion efficiency associated to the power losses caused by connecting cables, dc–dc and dc–ac conversion stages, sensing devices for protection, monitoring, and measuring purposes.
4) Another salient feature of CICERONE is that it operates without using external signals coming from sensors and usually affected by measuring noise (such as PV voltage, PV current, grid current, or their derivatives). Instead, it performs the MPPT using only an internal signal G_P, i.e., a signal already used for PFC purposes. Apart from the fact that no additional MPPT sensors are required, the use of the internal power factor correction signal means that such a signal is nearly unaffected by noise and other disturbances, and hence, the probability of occurrence of unpredictable MPPT errors due to noise and external disturbances is nearly reduced to zero.
5) CICERONE does not require either time derivative computations (time derivatives usually enhance high frequency noise and attenuate lower frequencies) or PV power calculation, which are usually associated to an increased computational burden and possible discretization errors, which can be reduced only by using ADC sensor circuits with quite high resolutions and, hence, high cost.

It is interesting to underline that, like the MPPT technique proposed in [16] and called T4S, CICERONE automatically takes into account the power stage efficiency profile. However, while T4S MPPT is devoted only to SS-GPVSs, CICERONE MPPT can be adopted without modifications for SS-GPVSs and DS-GPVSs, providing the bulk voltage reference signal for both kind of systems. Moreover, while as stated CICERONE only uses the internal PFC signal G_P, T4S in addition to G_P also needs an external signal (a scaled and low pass filtered

version of the PV voltage). Another aspect, which is worth noting is that T4S needs the computation of the time derivative of both the signal G_P and the bulk voltage, while CICERONE does not use time derivatives at all. Finally, in [16], only a preliminary numerical analysis of T4S is reported. In this article, CICERONE is validated in the laboratory and experimentally compared with the benchmark P&O technique by adopting the standard EN 50530 irradiance profile currently adopted just for testing inverter dynamic efficiency and MPPT algorithms [19], [20].

The rest of this article is organized as follows. In Section II, CICERONE based SS-GPVSs and DS-GPVSs are described in detail. In Section III, the operating principle of CICERONE MPPT technique is described. In Section IV, experimental results are shown. Finally, Section V concludes this article.

II. CICERONE Based Grid-Connected PV System

In Fig. 1, the block diagrams of traditional SS-GPVSs and DS-GPVSs are shown. Instead, in Fig. 2, the block diagram of the proposed CICERONE based grid-connected PV systems is reported. In particular, the block diagram of Fig. 2 is completely general since it can represent both SS-GPVSs and DS-GPVSs. In fact, the block "dc subsystem" in Fig. 2 represents the PV array in the case of a SS-GPVS or the PV array with the dc–dc converter (operating with a fixed duty-cycle) in the case of a DS-GPVS. The dc–ac converter control circuitry is based on two control loops: an inner current control loop aimed at the PFC and an outer voltage control loop aimed at the MPPT [12]. In particular, the internal current control loop must have a wide bandwidth since it performs the active control of the current injected into the grid in order to guarantee a power factor ideally equal to one. The outer voltage control loop employs a low-bandwidth controller for regulating the bulk capacitor voltage and, at the same time, allowing its oscillations at the second harmonic of the grid frequency. A wide variety of approaches can be adopted in order to accomplish these tasks and the details about the design of the system control loops are out of the scope of this article and can be found in [18]. It is possible to state that there is no conceptual difference among control loops in Figs. 1 and 2, and they can be designed on the basis of the same usual approaches [18]. However, by comparing Figs. 1 and 2, it is possible to observe that they differ for the MPPT control input signals. In fact, while traditional MPPT architectures (see Fig. 1) require, as input, signals that are external to the MPPT controller, only the internal signal G_P, already used for PFC purposes, is required by CICERONE MPPT controller (see Fig. 2). This is a salient feature of CICERONE since, while signals coming from external sensors are usually affected by measuring noise or other disturbances, internal signals are nearly devoid of those. Therefore, the probability of the occurrence of unpredictable MPPT errors due to noise and external disturbances is nearly reduced to zero.

In order to describe the operating principle of CICERONE MPPT technique, an ideal working of the internal current loop will be assumed, i.e.,

$$H_i \cdot i_{ac}\ (t) = i_{REF}\ (t) = G_P\ (t) \cdot v_{ac}\,(t) \tag{1}$$

where $i_{ac}(t)$ is the current injected into the grid, H_i is the gain of the sensor measuring $i_{ac}(t)$, and $i_{REF}(t)$ is the reference for the grid current. In order to guarantee a unit power factor, $i_{REF}(t)$ is obtained by multiplying the slowly time-varying gain $G_P(t)$ [Ω^{-1}] with the grid voltage $v_{ac}\ (t) = \sqrt{2}\ \cdot V_{ac} \cdot \sin\,(2\pi f_{ac} \cdot t)$, f_{ac} is the line frequency. Based on (1), the root mean square (rms) value I_{ac} of $i_{ac}(t)$ is equal to

$$I_{ac} = \frac{G_P\,(t) \cdot V_{ac}}{H_i} \tag{2}$$

and, hence, the active power injected into the grid is

$$P_{ac} = V_{ac}\ \cdot\ I_{ac} = \frac{G_P\,(t)}{H_i}\ \cdot V_{ac}^2. \tag{3}$$

Therefore, $G_P(t)$ regulates the average power P_{ac} injected into the grid. $G_P(t)$ is the output of the low-bandwidth voltage controller and, in order to avoid harmonics in the current injected into the grid, it must be a slowly time-varying signal [18]. In any case, the external voltage control loop, which is aimed at the proper regulation of the voltage $V_{BULK}(t)$, must have a limited bandwidth in order to allow the oscillation at $2 \cdot f_{ac}$ of $V_{BULK}(t)$, which is necessary for power balance purposes. The objective of the voltage control loop is to obtain the equality $H_v \cdot V_{BULK}\ (t) = H_v\ \cdot V_{REF}(t)$ where H_v is the voltage sensor gain. The reference voltage $H_v \cdot V_{REF}(t)$ for $H_v \cdot V_{BULK}(t)$ is provided, as shown in Fig. 2, by the CICERONE MPPT controller on the basis of the operating principle described in the following section.

III. CICERONE Operating Principle

As already stated, $G_P(t)$ is a slowly-varying signal [12] that, as shown by (3), dictates the value of the average power P_{ac}. On the basis of such a consideration, the objective of CICERONE MPPT technique is represented just by the identification of the proper reference voltage $H_v \cdot V_{REF}(t)$ for $H_v \cdot V_{BULK}(t)$ that leads to the maximization of $G_P(t)$ and, hence, of P_{ac}. As it is shown in Fig. 3, the operation of CICERONE is dictated by the two intervals of time called ΔT and T_{END} (with $\Delta T < T_{END}$). T_{END} is the period of CICERONE and ΔT is the interval of time needed to get a steady state operation of G_P in response to a ramp variation of V_{REF}. In particular, the operating principle of CICERONE is described by the following control law:

$$V_{REF}(t) = V_0\ + \int_0^t \sigma_{RAMP} \cdot \text{sign}\,\{\Delta V_{REF}\,(\tau)\,\Delta G_P\,(\tau)\} \cdot d\tau \tag{4}$$

where V_0 is the initial value of $V_{REF}(t)$, σ_{RAMP} [V/s] is a positive constant dictating the amplitude of the slope of $V_{REF}(t)$. Moreover, $\forall \tau \in [n \cdot T_{END}; (n+1) \cdot T_{END}]$ with $n\ =\ 1,\ 2,\ 3, \ldots$, it is

$$\Delta V_{REF}(\tau) = V_{REF}\ (n \cdot T_{END}) - V_{REF}\,((n-1) \cdot T_{END} + \Delta T) \tag{5.1}$$

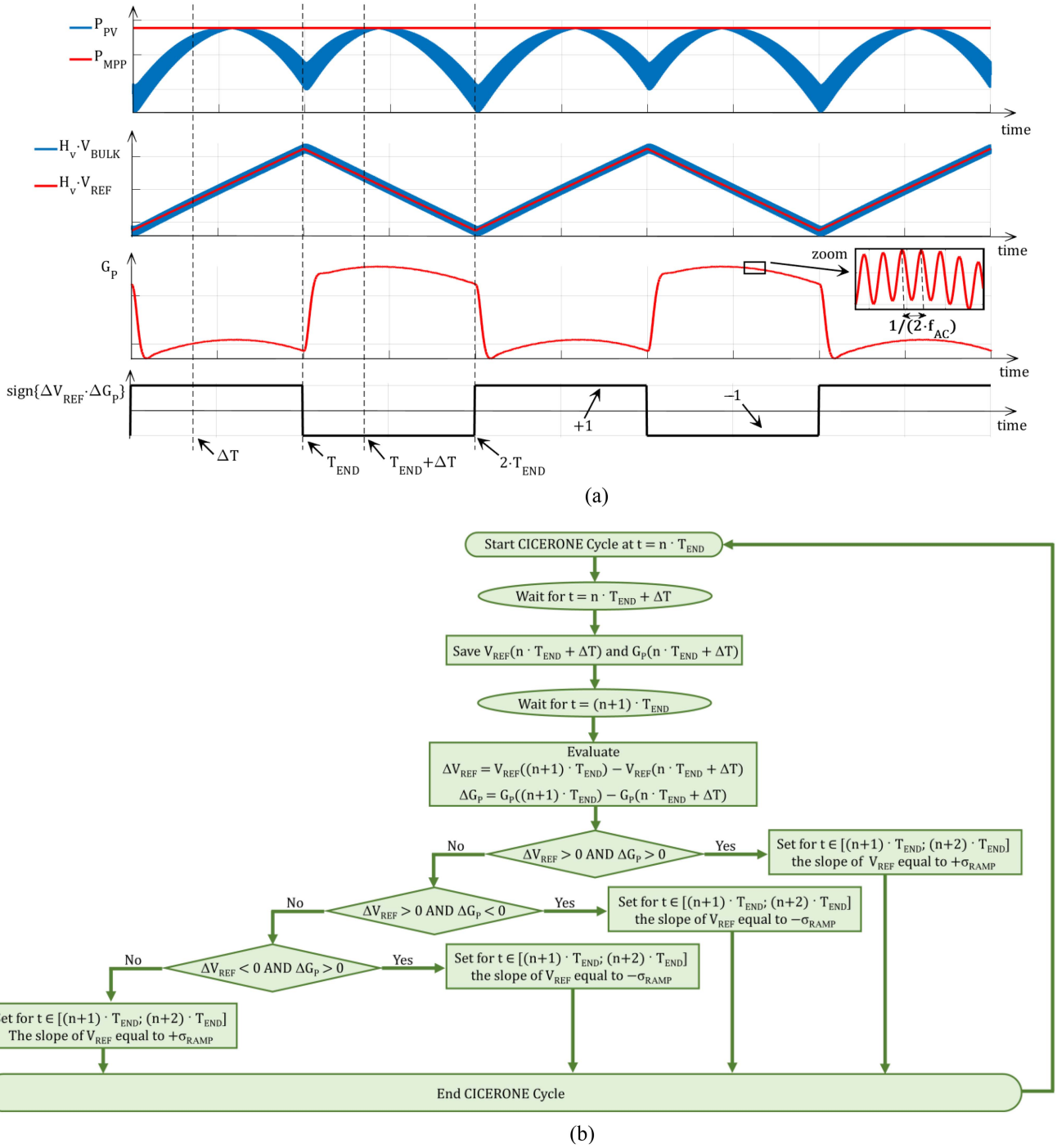

Fig. 3. (a) Qualitative trend of the waveforms in CICERONE MPPT controller. (b) CICERONE MPPT flow chart.

$$\Delta G_P\ (\tau) = G_P\ (n \cdot T_{END}) - G_P\left((n-1) \cdot T_{END} + \Delta T\right). \tag{5.2}$$

Equation (4) states that CICERONE MPPT controller generates the reference for the bulk voltage by integrating a signal whose absolute value is the constant σ_{RAMP} and whose sign is updated every T_{END} seconds according to the sign of the product between ΔV_{REF} and ΔG_P. In particular, $V_{REF}(t)$ is a ramp function characterized by a slope equal to $\pm\sigma_{RAMP}$.

In practice, as it is explained in the flow chart in Fig. 3(b), $V_{REF}(t)$ will have a positive slope $+\sigma_{RAMP}$ during $[n \cdot T_{END}; (n+1) \cdot T_{END}]$ if $V_{REF}(n \cdot T_{END}) > V_{REF}((n-1) \cdot T_{END} + \Delta T)$ and $G_P(n \cdot T_{END}) > G_P((n-1) \cdot T_{END} + \Delta T)$ or if $V_{REF}(n \cdot T_{END}) < V_{REF}((n-1) \cdot T_{END} + \Delta T)$ and $G_P(n \cdot T_{END}) < G_P((n-1) \cdot T_{END} + \Delta T)$. In other words, the slope of $V_{REF}(t)$ will be positive during $[n \cdot T_{END}; (n+1) \cdot T_{END}]$, only if V_{REF} and G_P have both increased or both decreased from $(n-1) \cdot T_{END} + \Delta T$ to $n \cdot T_{END}$. In fact, if G_P (and, hence, P_{ac}) has increased

with an increasing V_{REF}, or if G_P has decreased with a decreasing V_{REF}, then it means that the operating point is located at the left of the MPP and the MPPT direction for V_{REF} (the one leading to an increasing of G_P and, hence, of P_{ac}) is the increasing one. Similarly, the CICERONE output ramp signal will have a negative slope $-\sigma_{RAMP}$ during $[n \cdot T_{END}; (n+1) \cdot T_{END}]$ if $V_{REF}(n \cdot T_{END}) < V_{REF}((n-1) \cdot T_{END} + \Delta T)$ and $G_P(n \cdot T_{END}) > G_P((n-1) \cdot T_{END} + \Delta T)$ or if $V_{REF}(n \cdot T_{END}) > V_{REF}((n-1) \cdot T_{END} + \Delta T)$ and $G_P(n \cdot T_{END}) < G_P((n-1) \cdot T_{END} + \Delta T)$. In other words, the slope of $V_{REF}(t)$ will be negative during $[n \cdot T_{END}; (n+1) \cdot T_{END}]$, only if G_P has decreased with an increasing V_{REF}, or if G_P has increased with a decreasing V_{REF}. In this case, the MPPT direction for V_{REF} is the decreasing one since the operating point is located at the right of the MPP.

As it is shown in Fig. 3(a), at the steady state, in the neighborhood of the MPP, CICERONE leads to a V_{REF} waveform characterized by a piecewise ramp profile whose characteristics are strictly linked to the values assumed by the three parameters: σ_{RAMP}, ΔT, and T_{END}. Hence, the choice of such parameters is of fundamental importance and must be carefully carried out.

ΔT must be chosen by considering that, after every slope update of $V_{REF}(t)$, it will be possible to begin to measure ΔV_{REF} and ΔG_P only when the signal $V_{BULK}(t)$ has reached a steady state condition. Therefore, ΔT must be greater than the settling time of $V_{BULK}(t)$, i.e.,

$$\Delta T > T_{\varepsilon\%}^{RAMP} \tag{6}$$

where $T_{\varepsilon\%}^{RAMP}$ is the settling time at the $\varepsilon\%$ of the ramp response of the transfer function $W_{Vbulk\_Vref}(s)$ between $\hat{V}_{BULK}(s)$ and $\hat{V}_{REF}(s)$ [18].

As concerns T_{END}, it can be chosen on the basis of the following considerations. Since the external voltage control loop has a limited bandwidth, as it is shown in Fig. 3(a), the signal G_P is affected by a residual oscillation at $2 \cdot f_{ac}$. Therefore, in order to avoid errors in the measurement of ΔG_P due to such an oscillation, the interval of time $T_{END} - \Delta T$ on which ΔG_P is evaluated must be an integer multiple of the period of the frequency $2 \cdot f_{ac}$. Therefore, it must be

$$T_{END} = \Delta T + \frac{k}{2 \cdot f_{ac}} \tag{7}$$

where $k = 1, 2, 3, \ldots$ At least in principle, CICERONE is able to operate even with $k = 1$ but, in order to gain greater robustness, $k > 1$ can be chosen as it happens for the qualitative waveforms shown in Fig. 3(a).

With reference to σ_{RAMP}, it is worth noting that, in case of stationary irradiance conditions, any value of σ_{RAMP} high enough to overcome the switching noise, makes CICERONE able to reach the MPP provided that (6) and (7) are fulfilled. Instead, in time-varying irradiance conditions, the higher σ_{RAMP} the higher the peak–peak amplitude ΔV of every ramp of $V_{BULK}(t)$ and, hence, the higher the speed of tracking. However, at the same time, the higher σ_{RAMP} the lower the MPPT steady state efficiency (due to higher ΔV). Therefore, for the proper choice of σ_{RAMP}, a suitable compromise between speed of tracking and MPPT efficiency can be identified with reference to the desired time-variable irradiance profile. In particular, the value of σ_{RAMP} can be chosen on the basis of the following additional considerations.

Let us assume that the irradiance level has a variation ΔS during the interval of time with duration $T_{END} - \Delta T$. In particular, without any loss of generality, let us consider a starting value of the irradiance level (at $t = \Delta T$) equal to $S_i = S_{STC} = 1000\ W/m^2$ and a final value (at $t = T_{END}$) equal to $S_f = S_{STC} + \Delta S$. Given the maximum time derivative $dS/dt|_{MAX}$ of the irradiance that the system must be able to track, ΔS can be written as

$$\Delta S = \left.\frac{dS}{dt}\right|_{MAX} \cdot (T_{END} - \Delta T) = \left.\frac{dS}{dt}\right|_{MAX} \cdot \frac{k}{2 \cdot f_{ac}}. \tag{8}$$

Moreover, let us assume that the bulk voltage $V_{BULK}(t)$, due to CICERONE MPPT controller, has a variation ΔV during the interval of time with duration $T_{END} - \Delta T$. In particular, without any loss of generality, let us consider a starting value of V_{BULK} (at $t = \Delta T$) equal to $V_i = V_{MPP}$ (the STC MPP bulk voltage) and a final value (at $t = T_{END}$) equal to $V_f = V_{MPP} + \Delta V$. Given the ideal operation of the voltage controller, ΔV can be written as

$$\Delta V = \Delta V_{REF} = \sigma_{RAMP} \cdot (T_{END} - \Delta T) = \frac{\sigma_{RAMP} \cdot k}{2 \cdot f_{ac}}. \tag{9}$$

In such a case, in order to guarantee that CICERONE MPPT technique is not deceived, the variation of G_P that is due to ΔV, called $\Delta G_P|_{\Delta V}$, must be greater than the variation of G_P that is due to ΔS, called $\Delta G_P|_{\Delta S}$, i.e.,

$$|\Delta G_P|_{\Delta V}| > |\Delta G_P|_{\Delta S}|. \tag{10}$$

By considering the proportionality, expressed by (3), between G_P and the active power P_{ac} injected into the grid, (10) is equivalent to

$$|\Delta P_{ac}|_{\Delta V}| > |\Delta P_{ac}|_{\Delta S}| \tag{11}$$

where $\Delta P_{ac}|_{\Delta V}$ is the variation of P_{ac} due to ΔV and $\Delta P_{ac}|_{\Delta S}$ is the variation of P_{ac} due to ΔS. The two terms appearing in (11) can be identified on the basis of the following considerations. It is possible to write the expression of the variation ΔP_{PV} of the power provided by the dc-subsystem during the interval of time with duration $T_{END} - \Delta T$ as

$$\Delta P_{PV} = P_{PV}(V_f, S_f) - P_{PV}(V_i, S_i). \tag{12}$$

In particular, it is

$$P_{PV}(V_i, S_i) = P_{PV}(V_{MPP}, S_{STC}) = V_{MPP} \cdot I_{MPP} = P_{MPP} \tag{13}$$

where I_{MPP} is the STC MPP current at the output of the dc-subsystem, and it is

$$P_{PV}(V_f, S_f) = P_{PV}(V_{MPP} + \Delta V, S_{STC} + \Delta S) = \\ = (V_{MPP} + \Delta V) \cdot \left(I_{MPP} + I_{MPP} \cdot \frac{\Delta S}{S_{STC}}\right). \tag{14}$$

The expression (14) has been written by considering that, during an irradiance variation ΔS, the MPP current only changes

linearly with S. On the basis of (13) and (14), it can be written

$$\Delta P_{PV} = (V_{MPP} + \cdot V) \cdot \left(I_{MPP} + I_{MPP}\frac{\Delta S}{S_{STC}}\right) - P_{MPP} = \\ = \Delta V \cdot I_{MPP} + (V_{MPP} + \Delta V) \cdot I_{MPP}\frac{\Delta S}{S_{STC}}. \quad (15)$$

By taking into account the presence of the bulk capacitor C_{BULK} it is possible to obtain

$$\Delta P_{AC} = \Delta P_{PV} - \frac{1}{2}\frac{C_{BULK}}{T_{END}-\Delta T} \cdot \left(V_f^2 - V_i^2\right) = \\ = \Delta V \cdot I_{MPP} + (V_{MPP} + \Delta V) \cdot I_{MPP}\frac{\Delta S}{S_{STC}} + \\ - \frac{1}{2}\frac{C_{BULK}}{T_{END}-\Delta T} \cdot \left[(V_{MPP} + \Delta V)^2 - V_{MPP}^2\right]. \quad (16)$$

In the expression (16), it is possible to identify a term that depends only on ΔV, which is just $\Delta P_{ac}|_{\Delta V}$, i.e.,

$$\Delta P_{ac}|_{\Delta V} = \Delta V \cdot \left[I_{MPP} - \frac{1}{2}\frac{C_{BULK}}{T_{END} - \Delta T}(2V_{MPP} + \Delta V)\right]. \quad (17)$$

Moreover, in the expression (16), it is possible to identify a term that depends on ΔS, which is just $\Delta P_{ac}|_{\Delta S}$, i.e.,

$$\Delta P_{ac}|_{\Delta S} = (V_{MPP} + \Delta V) \cdot I_{MPP}\frac{\Delta S}{S_{STC}}. \quad (18)$$

Hence, on the basis of (17) and (18), and by taking into account the expression of ΔV given by (9), it is possible to identify the minimum value σ_{RAMP}^{min} of σ_{RAMP} that satisfies the inequality (11). All the values of σ_{RAMP} larger than σ_{RAMP}^{min} ensure that CICERONE MPPT technique is not deceived in presence of the considered time-variable irradiance conditions.

IV. Experimental Results

In this section, CICERONE MPPT technique is experimentally tested, and its performance is compared with that of the standard P&O MPPT technique in presence of different irradiance conditions. On the basis of the unified modeling of both SS-GPVSs and DS-GPVSs in Fig. 2, CICERONE can be applied without modifications to both SS-GPVSs and DS-GPVSs provided that, in the DS-GPVSs case, the dc–dc converter is operated with a fixed duty-cycle. Therefore, without any loss of generality and also due to some laboratory constraints, experimental tests were carried out on a 60 W nominal power SS-GPVS. A photo of the experimental setup is shown in Fig. 4(a) and the details of the laboratory prototype are reported in Tables I and II. In particular, in order to guarantee a fair comparison between CICERONE and P&O, a PV emulator was used instead of an actual PV source, to be able to compare the performance of the two MPPT techniques exactly in the same irradiance scenarios. This is of course impossible to obtain by using real PV sources, since the external climatic conditions are not controllable [23], [24], [25]. The power versus voltage characteristics of the emulated PV panel are reported in Fig. 4(b) for two different irradiance conditions (S = 1000 W/m^2 and S = 300 W/m^2). As it is shown in Fig. 4(a), the PV emulator uses a current-controlled linear power amplifier (OPA549) as the key element to emulate the PV panel.

A dedicated Arduino DUE board continuously senses the voltage $V_{BULK}(t)$ across the capacitor C_{BULK} and generates

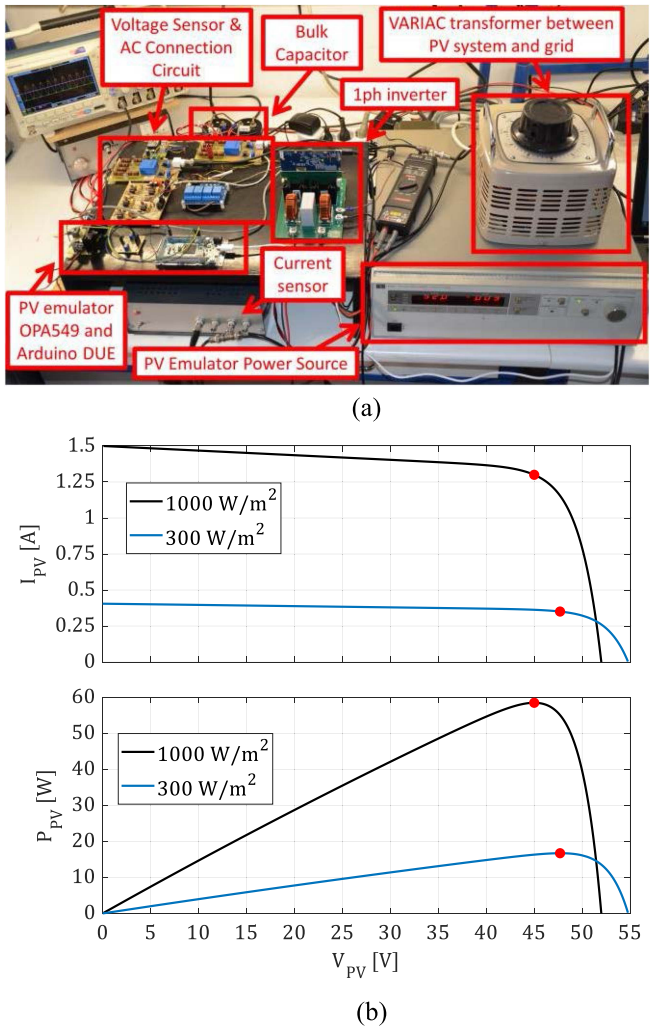

Fig. 4. (a) Photo of the experimental setup. (b) Current and power versus voltage characteristics of the emulated PV panel for two different irradiance conditions.

TABLE I
Prototype Components

Name	Parameter	Test condition	Value
Switch TPH3206PSB 180 mΩ GaN FET	V_{DS}	Tj ⊆ [–55 .. 150] °C	650 V
	I_c	Tc = 100 °C	10 A
		Tc = 25 °C	16 A
Switch Driver Si8233	f_{sw}		100 kHz
Ac side	L_{FILTER}		590 μH
	C_{FILTER}		2 μF
	V_{ac_rms}		18 V
PV side	C_{BULK}		10 mF

an analogue reference for the OPA549 based on the irradiance intensity level that is set in a LabView program. The OPA549 input voltage is obtained by using the controlled power supply HP 6035A. Moreover, a NI PXI-6115 was used to acquire the output of the voltage and current sensors on both the dc and

TABLE II
TEST SETUP AND ACQUISITION

Name	Identifier	Properties	Nominal Value
PV Emulator	HP 6030A	Fixed voltage	55 V
	OPA549	Current controlled	10 A
	ARDUINO DUE	Lookup table	10 kHz
Ac side sensors	LEM LA25-P	Current sensing	25 A
	LEM LV25-P	Voltage sensing	60 V
PV side sensors	LEM LA25-P	Current sensing	25 A
	LEM LV25-P	Voltage sensing	60 V
Data Acquisition system	NI PXI-6115	4 simultaneous AI	12 bit 10 MS/s/ch

ac sides. The voltage and current controllers, and the MPPT algorithms (CICERONE or P&O), run on a Delfino C2000 DSP board (TMDSCNCD28379D based controlCARD). Oversampling methods and averaging were used to minimize the effects of the measurement noise. The implemented system was not directly connected to the main grid but, in order to obtain a scaled grid voltage with an rms value equal to 18 V, a variac was placed between the implemented system and the main grid.

The value of the capacitance C_{BULK}, reported in Table I, was chosen on the basis of the following considerations aimed at guarantee that the system is not deceived by the oscillation of $V_{BULK}(t)$ at $2 \cdot f_{ac}$, which is necessary for power balance purposes and whose peak to peak amplitude is [12]

$$\Delta V_{100} = \frac{P_{MPP}}{V_{MPP} \cdot C_{BULK} \cdot 2\pi f_{ac}}. \tag{19}$$

In particular, the variation of G_P that is due to ΔV, called $\Delta G_P|_{\Delta V}$, must be greater than the variation of G_P that is due to ΔV_{100}, called $\Delta G_P|_{\Delta V_{100}}$, i.e.,

$$|\Delta G_P|_{\Delta V}| > |\Delta G_P|_{\Delta V_{100}}|. \tag{20}$$

By considering the proportionality, expressed by (3), between G_P and the active power P_{ac} injected into the grid, (20) is equivalent to

$$|\Delta P_{ac}|_{\Delta V}| > |\Delta P_{ac}|_{\Delta V_{100}}| \tag{21}$$

where $\Delta P_{ac}|_{\Delta V}$ is the variation of P_{ac} due to ΔV and $\Delta P_{ac}|_{\Delta V_{100}}$ is the variation of P_{ac} due to ΔV_{100}.

In order to guarantee both (11) and (21), the following inequality can be fulfilled:

$$|\Delta P_{ac}|_{\Delta V}| > |\Delta P_{ac}|_{\Delta S}| > |\Delta P_{ac}|_{\Delta V_{100}}|. \tag{22}$$

Therefore, on the basis of (22), inequality (23) is surely satisfied

$$|\Delta P_{ac}|_{\Delta S}| > |\Delta P_{ac}|_{\Delta V_{100}}|. \tag{23}$$

The term $\Delta P_{ac}|_{\Delta V_{100}}$ can be evaluated by substituting $\Delta V = \Delta V_{100}$ in (17), obtaining

$$\Delta P_{ac}|_{\Delta V_{100}} = \Delta V_{100} \cdot I_{MPP} + - \frac{1}{2}\Delta V_{100} \cdot \frac{C_{BULK}}{T_{END} - \Delta T}(2V_{MPP} + \Delta V_{100}). \tag{24}$$

The minimum value of the term $\Delta P_{ac}|_{\Delta S}$ can be obtained by substituting $\Delta V = 0$ in (18), obtaining

$$\Delta P_{ac}|_{\Delta S} = V_{MPP} \cdot I_{MPP}\frac{\Delta S}{S_{STC}}. \tag{25}$$

Hence, by substituting (24) and (25) in inequality (23), it is possible to obtain the minimum value of C_{BULK} that is

$$C_{BULK}^{min} = \frac{I_{MPP} \cdot S_{STC}}{V_{MPP} \cdot 4\pi f_{ac}} \frac{4\pi f_{ac}(T_{END} - \Delta T) - 1}{2\pi f_{ac} \cdot \Delta S(T_{END} - \Delta T) + S_{STC}}. \tag{26}$$

By considering, as it is shown in Fig. 4(b), for $S = 1000\ W/m^2$, $I_{MPP} = 1.3\ A$, and $V_{MPP} = 45\ V$ and by choosing, on the basis of the consideration reported in the previous section, $T_{END} = 0.35\ s$ and $\Delta T = 0.15\ s$ (sufficiently larger than the system settling time at the 1%), (26) leads to $C_{BULK}^{min} = 2.6\ mF$. Hence, $C_{BULK} = 10\ mF$, which is sufficiently larger than C_{BULK}^{min}, has been chosen as reported in Table I.

In the following sections, the tests that were carried out are described in details.

A. CICERONE Under Stationary Irradiance Conditions

The first part of the experimental tests was carried out by considering two different stationary irradiance conditions 1000 W/m^2 and 300 W/m^2. CICERONE MPPT technique was tested with different values of σ_{RAMP} that lead to different values of ΔV_{RAMP}

$$\Delta V_{RAMP} = \sigma_{RAMP} \cdot T_{END}. \tag{27}$$

In particular, as it has been shown in the previous section, on the basis of (17) and (18), and by taking into account the expression of ΔV given by (9), it is possible to identify the minimum value σ_{RAMP}^{min} of σ_{RAMP} that satisfies the inequality (11). By considering $T_{END} = 0.35\ s$, $\Delta T = 0.15\ s$, $C_{BULK} = 10\ mF$, $I_{MPP} = 1.3\ A$, $V_{MPP} = 45\ V$, and $dS/dt|_{MAX} = 100\ W/m^2/s$ (the largest used slope in the standard EN 50530 that will be considered in the dynamic test of the following section), it is $\sigma_{RAMP}^{min} \cong 6.6\ V/s$ corresponding to a $\Delta V_{RAMP}^{min} \cong 2.3\ V$. Therefore, CICERONE MPPT technique was tested with different values of σ_{RAMP} both smaller and larger than σ_{RAMP}^{min}, leading to different values of ΔV_{RAMP} (ranging from $\Delta V_{RAMP} = 0.5\ V$ to $\Delta V_{RAMP} = 10\ V$) both smaller and larger than ΔV_{RAMP}^{min}. In Fig. 5, the average power P_{ac} is reported for such values of ΔV_{RAMP} in presence of the two considered irradiance values.

It is possible to observe that, in both cases, there is a range of values of ΔV_{RAMP} for which the average extracted power is nearly the same and the highest one. In this optimal range, the values of ΔV_{RAMP} are small enough to cause a limited excursion of the operating point (distancing from the MPP) at the steady state but are high enough to overcome the switching

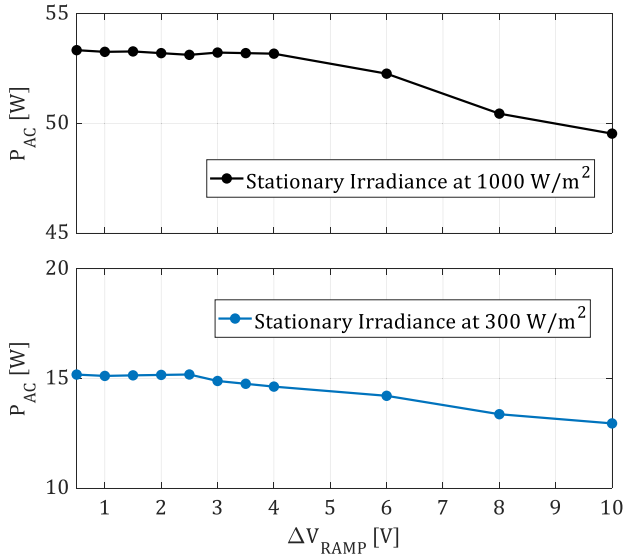

Fig. 5. Results of the test in presence of stationary irradiance conditions.

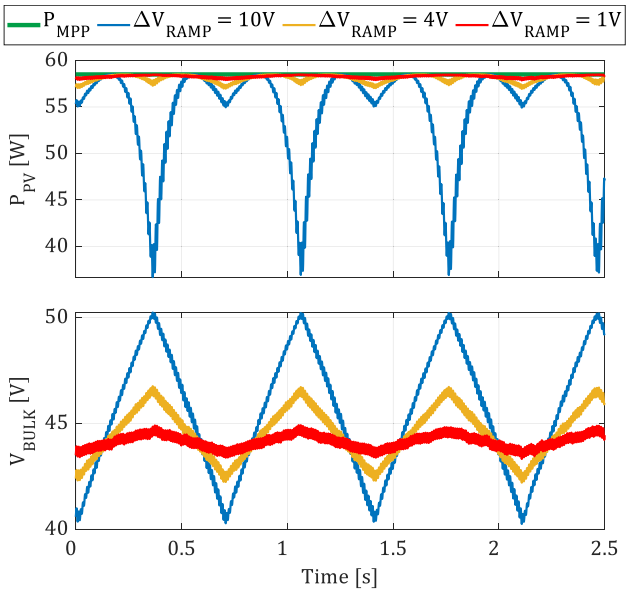

Fig. 6. Waveforms acquired in case of a stationary irradiance S = 1000 W/m^2 for different values of ΔV_{RAMP}.

noise. Of course, the average extracted power decreases for very high values of ΔV_{RAMP}, which unavoidably lead to large excursions of the operating point at the steady state. In fact, as it was explained in the previous section, in case of stationary irradiance conditions, any value of ΔV_{RAMP} high enough to overcome the switching noise, makes CICERONE able to reach the MPP. However, the higher ΔV_{RAMP} the lower the MPPT steady state efficiency.

These considerations are confirmed by Figs. 6 and 7, which show the waveforms of the instantaneous PV power P_{PV} and of the bulk voltage V_{BULK} for three different values of ΔV_{RAMP}. In particular, in Fig. 6 the waveforms acquired in case of a stationary irradiance equal to 1000 W/m^2 are reported, and in Fig. 7 those ones in the case of 300 W/m^2 are reported. The

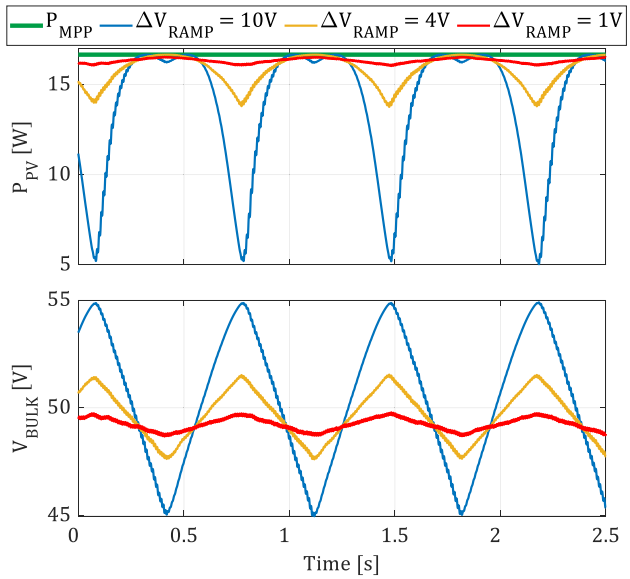

Fig. 7. Waveforms acquired in case of a stationary irradiance S = 300 W/m^2 for different values of ΔV_{RAMP}.

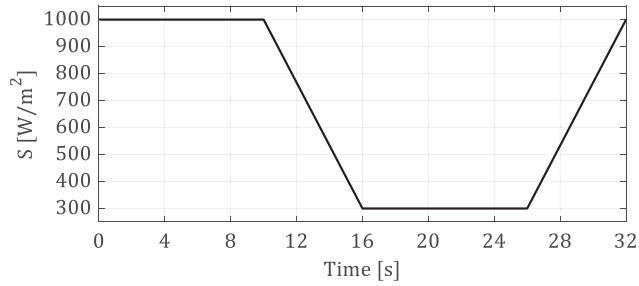

Fig. 8. Considered time-variable irradiance profile.

negative effect of the choice of a too large value of ΔV_{RAMP} is evident. In fact, by increasing ΔV_{RAMP}, even if the system becomes faster and generally more robust to noise effects, the excursion of the operating point from the MPP is so large that the average extracted power is strongly reduced.

This is a kind of behavior that is very similar to that of the P&O but, as it will be shown in the following, CICERONE is generally more robust. Instead, in time-varying irradiance conditions, as it will be shown in the following section, ΔV_{RAMP} should be the result of a suitable compromise between speed of tracking and MPPT efficiency leading to the choice of ΔV_{RAMP}^{min} taking into account the desired time-variable irradiance profile.

B. CICERONE Under Variable Irradiance Conditions

The second set of the experimental tests was carried out by considering the time-variable irradiance profile that is shown in Fig. 8. Such an irradiance profile was chosen according to the standard EN 50530 for testing inverter dynamic efficiency and MPPT algorithms [19], [20]. In particular, it is characterized by two excursions (one decreasing and one increasing) between two irradiance levels (1000 W/m^2 and 300 W/m^2). Such excursions have ramp profiles with a slope equal to about 100 W/m^2/s, which is the biggest considered slope in the standard EN 50530.

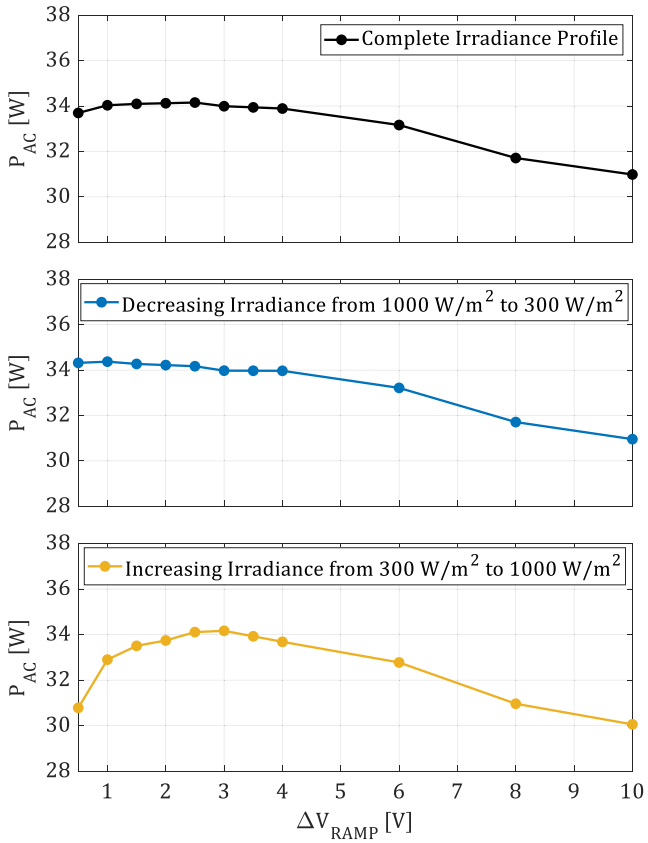

Fig. 9. Results of the test in presence of time-variable irradiance conditions.

Also in this case, CICERONE MPPT technique was tested with different values of ΔV_{RAMP}, and in Fig. 9, the average power P_{ac} is reported as a function of ΔV_{RAMP}. In particular, the graphs in Fig. 9(black curve) show the results for the complete irradiance profile (that one in Fig. 8) together with the results obtained either in the part of the profile characterized by a decreasing irradiance (from 1000 W/m^2 to 300 W/m^2, blue curve) or in the part of the profile characterized by an increasing irradiance (from 300 W/m^2 to 1000 W/m^2, yellow curve).

It is possible to note that, also for the case of the complete irradiance profile, there are values of ΔV_{RAMP} for which the average extracted power is nearly the same. This can be explained with the help of the waveforms shown in Fig. 10. In particular, with reference to $\Delta V_{RAMP} = 1$ V, even if with such a value of ΔV_{RAMP} smaller than ΔV_{RAMP}^{min} the system is deceived, the excursion from the MPP is so small that the average extracted power is only slightly lower than the middle case $\Delta V_{RAMP} = 4$ V (larger than ΔV_{RAMP}^{min}). This is verified also for the decreasing irradiance case, as it is evident from Fig. 11.

With reference to the case of an increasing irradiance profile, since in that case the irradiance variation tends to increase the extracted power, the system is less robust. This is exactly the same situation that happens for the P&O, as it will be shown in the following section. In particular, as it has been shown in the previous section, in order to avoid MPPT errors, the variation of the extracted power, which is a function of ΔV_{RAMP},

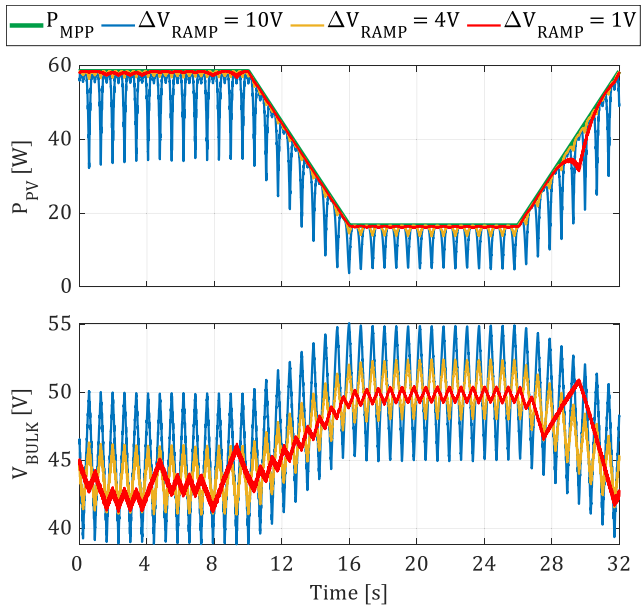

Fig. 10. Waveforms acquired in case of the time-variable irradiance profile shown in Fig. 8, for different values of ΔV_{RAMP}.

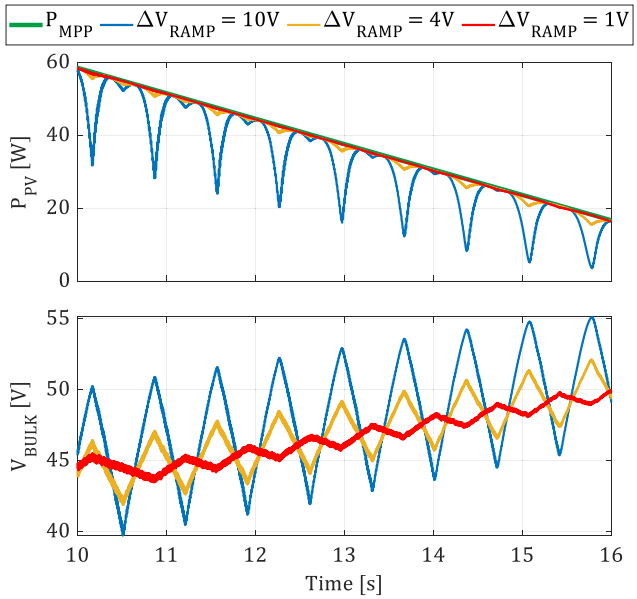

Fig. 11. Zoom of Fig. 10 showing the waveforms in case of decreasing irradiance profile from 1000 to 300 W/m^2 for different values of ΔV_{RAMP}.

must be greater than the variation of the extracted power due to the maximum irradiance variation. This is verified only for values of ΔV_{RAMP} that are larger than ΔV_{RAMP}^{min}. Moreover, as it is expected, an optimal range exists because when ΔV_{RAMP} assumes too large values, even if the system is very fast and not deceived, the excursion from the MPP is so big that the average extracted power is reduced. All these considerations are confirmed by Fig. 12, showing that for $\Delta V_{RAMP} = 1$ V the system is completely deceived and for $\Delta V_{RAMP} = 10$ V the power excursion is too big even if the system is not deceived. The case $\Delta V_{RAMP} = 4$ V can be considered a good compromise:

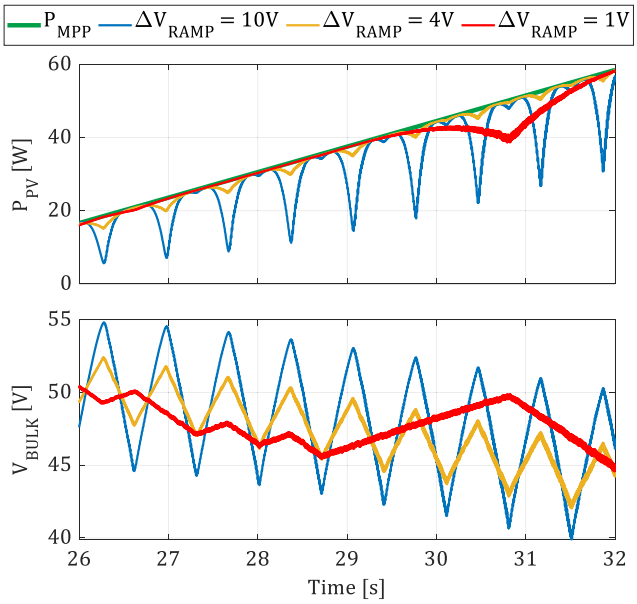

Fig. 12. Zoom of Fig. 10 showing the waveforms in case of increasing irradiance profile from 300 to 1000 W/m^2 for different values of ΔV_{RAMP}.

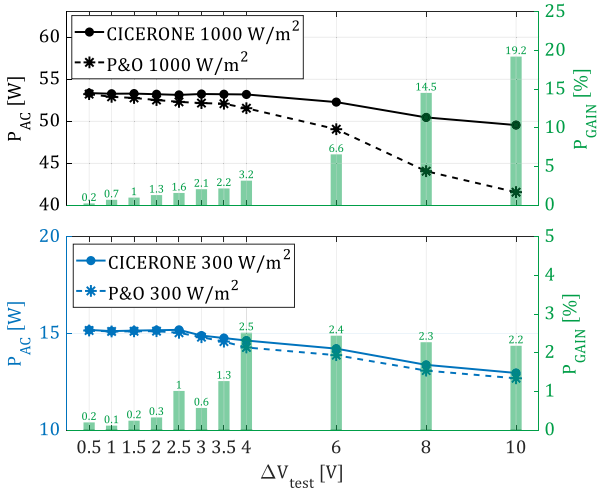

Fig. 13. Results of the test in presence of stationary irradiance conditions.

the excursion of power is enough large so that the system is not deceived but it is enough small to have good power performance.

C. Comparison of CICERONE and P&O

CICERONE MPPT algorithm can be inserted in the group of the "hill climbing" MPPT algorithms. In such a group, the P&O is one of the simplest but nonetheless more efficient and is widely considered as a benchmark for the other MPPT techniques [21], [22]. Therefore, the last set of experimental tests was carried out for comparing the performance of CICERONE with that of the P&O. Therefore, the previous results obtained with CICERONE were compared with the results obtained with the P&O, both in the case of stationary irradiance conditions and in the case of the time-variable irradiance profile (see Fig. 8). The performances of the two techniques are summarized and compared in Fig. 13, with reference to the stationary irradiance

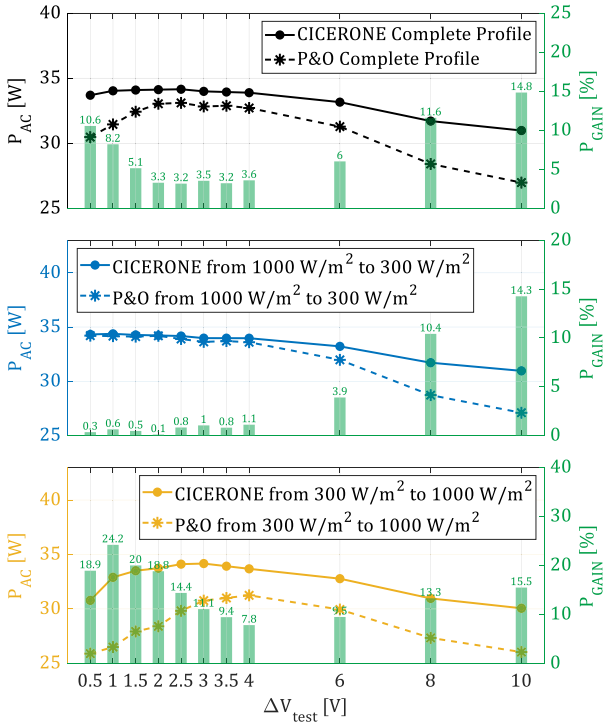

Fig. 14. Results of the test in presence of time-variable irradiance conditions.

values, and in Fig. 14, with reference to the dynamic irradiance conditions. In particular, such figures show (left vertical axis) the average extracted power P_{ac} for the two MPPT techniques and for different values of $\Delta V_{test} = \Delta V_{RAMP}$ for CICERONE and $\Delta V_{test} = \Delta V_{REF}$ (amplitude of the step perturbation of V_{REF}) for the P&O. Moreover, in the same figures also the percentage power gain P_{GAIN} that can be obtained with CICERONE with respect to the P&O is reported as a function of ΔV_{test}. In particular, such a power gain is defined as it follows:

$$P_{GAIN} = \frac{P_{ac\_CICERONE} - P_{ac\_P\&O}}{P_{ac\_P\&O}} \cdot 100\% \qquad (28)$$

where $P_{ac\_CICERONE}$ is the average extracted power with CICERONE and $P_{ac\_P\&O}$ is that with the P&O.

By looking at those figures it can be observed that, being both CICERONE and P&O hill climbing techniques, they are characterized by similar trends of P_{ac} versus ΔV_{test}. However, it can be noted that for every irradiance condition, CICERONE is characterized by a greater robustness as concerns the choice of ΔV_{test}. In fact, it is characterized by a larger range of values of ΔV_{test} for which the extracted power is nearly maximized.

Moreover, it is also evident that the behavior of CICERONE in dynamic irradiance conditions is better than that of the P&O, especially with reference to the most challenging case of increasing irradiance profile (see Fig. 14, yellow curves).

It is well known that, in presence of time-varying irradiance profiles, smart P&O strategies adapting the step size provide improved performances [26], [27], [28]. Similar strategies can be adopted also with reference to CICERONE adapting the ramp slope value. Undoubtedly, the possibility to choose the slope

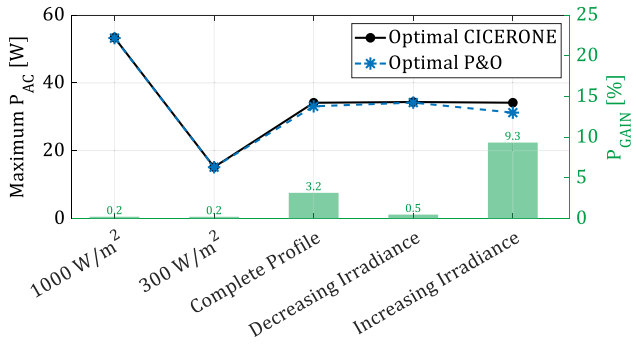

Fig. 15. Summary of all the tests.

value in a quite large range represents a valuable advantage of CICERONE in terms of robustness.

A summary of all the tests is shown in Fig. 15, where the optimal point of CICERONE is compared, for every considered irradiance condition, with the optimal one of the P&O. It can be observed that, in terms of extractable power the two techniques are nearly comparable in stationary irradiance conditions. CICERONE is, instead, able to extract a higher power in case of variable irradiance conditions with a maximum gain of power equal to about 9% in case of increasing irradiance.

V. Conclusion

In this article, a novel MPPT technique has been proposed. It is called CICERONE and it allows the tracking of the maximum average ac power automatically taking into account the dc–ac power stage efficiency profile in case of both SS and DS-GPVS. A very important feature of CICERONE is that it operates without using external signals coming from sensors and affected by measuring noise. It is able to perform the MPPT very robustly, exploiting only an internal signal already used for the necessary PFC control. Experimental tests have been carried out in order to compare the performances of CICERONE with those of the well-known and widespread used P&O, in different stationary and time-variable irradiance conditions. It is possible to state that CICERONE and P&O are characterized by similar trends of P_{ac} versus ΔV_{test} with comparable values of ac extracted power in stationary irradiance conditions. CICERONE is, instead, able to extract a higher power in case of variable irradiance conditions with a maximum gain of power equal to about 9% in case of increasing irradiance. Moreover, for every irradiance condition, CICERONE is characterized by a greater robustness as concerns the choice of ΔV_{test}, with a larger range of values for which the extracted power is nearly maximized.

References

[1] A. Allouhi, S. Rehman, M. S. Buker, and Z. Said, "Up-to-date literature review on Solar PV systems: Technology progress, market status and R&D," *J. Cleaner Prod.*, vol. 362, 2022, Art. no. 132339.

[2] O. O. Apeh, E. L. Meyer, and O. K. Overen, "Contributions of solar photovoltaic systems to environmental and socioeconomic aspects of national development—A review," *Energies*, vol. 15, no. 16, Aug. 2022, Art. no. 5963, doi: 10.3390/en15165963.

[3] L. Hernández-Callejo, S. Gallardo-Saavedra, and V. Alonso-Gómez, "A review of photovoltaic systems: Design, operation and maintenance," *Sol. Energy*, vol. 188, pp. 426–440, 2019.

[4] S. K. Sahoo, S. Sukchai, and F. F. Yanine, "Review and comparative study of single-stage inverters for a PV system," *Renewable Sustain. Energy Rev.*, vol. 91, pp. 962–986, 2018.

[5] X. Wang, F. Zhuo, J. Li, L. Wang, and S. Ni, "Modeling and control of dual-stage high-power multifunctional PV system in d - Q - o coordinate," *IEEE Trans. Ind. Electron.*, vol. 60, no. 4, pp. 1556–1570, Apr. 2013, doi: 10.1109/TIE.2012.2202349.

[6] F. Ronilaya et al., "A double stage micro-inverter for optimal power flow control in grid connected PV system," in *Proc. Int. Conf. Inf. Commun. Technol.*, Yogyakarta, Indonesia, 2018, pp. 808–813, doi: 10.1109/ICOIACT.2018.8350788.

[7] A. Laib, F. Krim, B. Talbi, A. Kihal, and A. Sahli, "Predictive control strategy for double-stage grid connected PV systems," in *Advanced Control Engineering Methods in Electrical Engineering Systems. ICEECA 2017. Lecture Notes in Electrical Engineering*, M. Chadli, S. Bououden, S. Ziani, and I. Zelinka, Eds., Cham, Switzerland: Springer, 2019, doi: 10.1007/978-3-319-97816-1_24.

[8] S. Jiang, D. Cao, Y. Li, and F. Z. Peng, "Grid-connected boost-half-bridge photovoltaic microinverter system using repetitive current control and maximum power point tracking," *IEEE Trans. Power Electron.*, vol. 27, no. 11, pp. 4711–4722, Nov. 2012, doi: 10.1109/TPEL.2012.2183389.

[9] H. Patel and V. Agarwal, "MPPT scheme for a PV-fed single-phase single-stage grid-connected inverter operating in CCM with only one current sensor," *IEEE Trans. Energy Convers.*, vol. 24, no. 1, pp. 256–263, Mar. 2009, doi: 10.1109/TEC.2008.2005282.

[10] F. Blaabjerg, R. Teodorescu, M. Liserre, and A. Timbus, "Overview of control and grid synchronization for distributed power generation systems," *IEEE Trans. Ind. Electron.*, vol. 53, no. 5, pp. 1398–1409, Oct. 2006.

[11] Y.-K. Lo, T.-P. Lee, and K.-H. Wu, "Grid-connected photovoltaic system with power factor correction," *IEEE Trans. Ind. Electron.*, vol. 55, no. 5, pp. 2224–2227, May 2008, doi: 10.1109/TIE.2008.921204.

[12] N. Femia, G. Petrone, G. Spagnuolo, and M. Vitelli, "A technique for improving P&O MPPT performances of double-stage grid-connected photovoltaic systems," *IEEE Trans. Ind. Electron.*, vol. 56, no. 11, pp. 4473–4482, Nov. 2009, doi: 10.1109/TIE.2009.2029589.

[13] H. Rezk and A. M. Eltamaly, "A comprehensive comparison of different MPPT techniques for photovoltaic systems," *Sol. Energy*, vol. 112, pp. 1–11, 2015.

[14] M. Balato, L. Costanzo, P. Marino, G. Rubino, L. Rubino, and M. Vitelli, "Modified TEODI MPPT technique: Theoretical analysis and experimental validation in uniform and mismatching conditions," *IEEE J. Photovolt.*, vol. 7, no. 2, pp. 604–613, Mar. 2017, doi: 10.1109/JPHOTOV.2016.2634327.

[15] M. L. Katche, A. B. Makokha, S. O. Zachary, and M. S. Adaramola, "A comprehensive review of maximum power point tracking (MPPT) techniques used in solar PV systems," *Energies*, vol. 16, no. 5, Feb. 2023, Art. no. 2206, doi: 10.3390/en16052206.

[16] Costanzo and Vitelli, "A novel MPPT technique for single stage grid-connected PV systems: T4S," *Energies*, vol. 12, no. 23, Nov. 2019, Art. no. 4501, doi: 10.3390/en12234501.

[17] L. Davila-Gomez, A. Colmenar-Santos, M. Tawfik, and M. Castro-Gil, "An accurate model for simulating energetic behavior of PV grid connected inverters," *Simul. Model. Pract. Theory*, vol. 49, pp. 57–72, 2014.

[18] R. W. Erickson and D. Maksimovic, *Fundamentals of Power Electronics*, 3nd ed. Springer Nature Switzerland AG, 2020, doi: 10.1007/978-3-030-43881-4.

[19] T. Andrejašič, M. Jankovec, and M. Topič, "Comparison of direct maximum power point tracking algorithms using EN 50530 dynamic test procedure," *IET Renewable Power Gener.*, vol. 5, no. 4, 2011, pp. 281–286.

[20] X. Li and H. Wen, "Evaluation of different maximum power point tracking techniques by using EN 50530 dynamic test standard," in *Proc. IEEE Int. Conf. Power Electron., Drives Energy Syst.*, Trivandrum, India, 2016, pp. 1–6, doi: 10.1109/PEDES.2016.7914246.

[21] N. Femia, G. Petrone, G. Spagnuolo, and M. Vitelli, "Optimization of perturb and observe maximum power point tracking method," *IEEE Trans. Power Electron.*, vol. 20, no. 4, pp. 963–973, Jul. 2005, doi: 10.1109/TPEL.2005.850975.

[22] L. Costanzo, A. L. Schiavo, and M. Vitelli, "Design guidelines for the Perturb and Observe Technique for electromagnetic vibration energy harvesters feeding bridge rectifiers," *IEEE Trans. Ind. Appl.*, vol. 55, no. 5, pp. 5089–5098, Sep./Oct. 2019, doi: 10.1109/TIA.2019.2923162.

[23] M. Balato, L. Costanzo, D. Gallo, C. Landi, M. Luiso, and M. Vitelli, "Design and implementation of a dynamic FPAA based photovoltaic emulator," *Sol. Energy*, vol. 123, pp. 102–115, Jan. 2016, doi: 10.1016/j.solener.2015.11.006.
[24] A. F. Ebrahim, S. M. W. Ahmed, S. E. Elmasry, and O. A. Mohammed, "Implementation of a PV emulator using programmable DC power supply," in *Proc. SoutheastCon*, Fort Lauderdale, FL, USA, 2015, pp. 1–7, doi: 10.1109/SECON.2015.7133048.
[25] A. Boucharef, A. Tahri, F. Tahri, S. Silvestre, and M. Bourahla, "Solar module emulator based on a low-cost microcontroller," *Measurement*, vol. 187, 2022, Art. no. 110275.
[26] N. Fermia, D. Granozio, G. Petrone, and M. Vitelli, "Predictive & adaptive MPPT perturb and observe method," *IEEE Trans. Aerosp. Electron. Syst.*, vol. 43, no. 3, pp. 934–950, Jul. 2007.
[27] D. Sera, R. Teodorescu, J. Hantschel, and M. Knoll, "Optimized maximum power point tracker for fast-changing environmental conditions," *IEEE Trans. Ind. Electron.*, vol. 55, no. 7, pp. 2629–2637, Jul. 2008, doi: 10.1109/TIE.2008.924036.
[28] M. Killi and S. Samanta, "An adaptive voltage-sensor-based MPPT for photovoltaic systems With SEPIC converter including steady-state and drift analysis," *IEEE Trans. Ind. Electron.*, vol. 62, no. 12, pp. 7609–7619, Dec. 2015.

Luigi Costanzo was born in Italy, in 1989. He received the master's degree (*cum laude*) in electronic engineering from the Second University of Naples, Naples, Italy, in 2014, and the Ph.D. degree in industrial and information engineering from the Department of Industrial and Information Engineering, Università degli Studi della Campania "Luigi Vanvitelli," Caserta, Italy, in 2017.

He is currently an Assistant Professor with the Department of Engineering, Università degli Studi della Campania "Luigi Vanvitelli." He has coauthored a number of national and international patents and research articles. His main research interests include maximum power point tracking techniques in photovoltaic applications, power electronics circuits for renewable energy sources, and analysis, design and optimization of energy harvesting systems.

Guido Rubino (Member, IEEE) received the M.S. degree in electronic engineering and the Ph.D. degree in energy conversion from the Department of Industrial and Information Engineering, University of Campania "Luigi Vanvitelli," Caserta, Italy, in 2011 and 2014, respectively.

He is a Researcher with the Department of Engineering, University of Rome "Sapienza," Rome, Italy, where his research activities focus on electronic power converters, electric machines, and drives. He has actively participated in numerous national and international science projects. His main research interests include the design of high power density power converters, electric drives, and control systems.

Dr. Rubino is actively contributes as a reviewer for various international scientific journals in the field of power electronics.

Luigi Rubino received the M.S. degree in electronic engineering and the Ph.D. degree in energy conversion from the Department of Industrial and Information Engineering, University of Campania "Luigi Vanvitelli," Caserta, Italy, in 2008 and 2012, respectively.

He is an Associate Professor with the University of Campania "Luigi Vanvitelli". His research activities focus on power electronic, electric machines, and drives. He has actively participated in numerous national and international research projects. His main research interests include run time optimization methods for onboard power management, digital control, high power density power converters, and solid state protection.

He is an IEEE Industrial Electronics Society member.

Massimo Vitelli was born in Caserta, Italy, in 1967. He received the laurea degree (*cum laude*) in electrical engineering from the University of Naples Federico II, Naples, Italy, in 1992.

He is currently a Full Professor with the Department of Engineering, Università degli Studi della Campania "Luigi Vanvitelli," Caserta, Italy, where he teaches electric circuits and power electronics. He was engaged in many scientific national projects. He has coauthored a number of national and international patents and two scientific books. His main research interests include maximum power point tracking techniques in photovoltaic applications, power electronics circuits for renewable energy sources, and methods for analysis, design and optimization energy harvesting systems.

Dr. Vitelli is an Associate Editor for IEEE TRANSACTIONS ON POWER ELECTRONICS.